Selective role for superoxide in $InsP_3$ receptor–mediated mitochondrial dysfunction and endothelial apoptosis

Muniswamy Madesh,[1,2] Brian J. Hawkins,[1] Tatyana Milovanova,[1] Cunnigaiper D. Bhanumathy,[3] Suresh K. Joseph,[3] Satish P. RamachandraRao,[4] Kumar Sharma,[4] Tomohiro Kurosaki,[5] and Aron B. Fisher[1]

[1]Institute for Environmental Medicine and [2]Department of Cancer Biology, University of Pennsylvania, Philadelphia, PA 19104
[3]Department of Pathology, Anatomy, and Cell Biology and [4]Dorrance Hamilton Research Laboratories, Thomas Jefferson University, Philadelphia, PA 19107
[5]Laboratory for Lymphocyte Differentiation, Institute of Physical and Chemical Research, Research Center for Allergy and Immunology, Turumi-ku, Yokohama 230-0045, Japan

Reactive oxygen species (ROS) play a divergent role in both cell survival and cell death during ischemia/reperfusion (I/R) injury and associated inflammation. In this study, ROS generation by activated macrophages evoked an intracellular Ca^{2+} ($[Ca^{2+}]_i$) transient in endothelial cells that was ablated by a combination of superoxide dismutase and an anion channel blocker. $[Ca^{2+}]_i$ store depletion, but not extracellular Ca^{2+} chelation, prevented $[Ca^{2+}]_i$ elevation in response to $O_2^{\cdot-}$ that was inositol 1,4,5-trisphosphate ($InsP_3$) dependent, and cells lacking the three $InsP_3$ receptor ($InsP_3R$) isoforms failed to display the $[Ca^{2+}]_i$ transient. Importantly, the $O_2^{\cdot-}$-triggered Ca^{2+} mobilization preceded a loss in mitochondrial membrane potential that was independent of other oxidants and mitochondrially derived ROS. Activation of apoptosis occurred selectively in response to $O_2^{\cdot-}$ and could be prevented by $[Ca^{2+}]_i$ buffering. This study provides evidence that $O_2^{\cdot-}$ facilitates an $InsP_3R$-linked apoptotic cascade and may serve a critical function in I/R injury and inflammation.

Introduction

Receptor-mediated generation of reactive oxygen species (ROS) is necessary for signal transduction, gene expression, and cell proliferation in smooth muscle cells, T and B lymphocytes, and fibroblasts (Devadas et al., 2002). Conversely, ROS produced under pathological conditions such as ischemia/reperfusion (I/R) or inflammation are associated with cellular dysfunction and apoptosis (Davies, 1995). Endothelial cells respond to numerous external stimuli by producing the superoxide anion ($O_2^{\cdot-}$). In physiological conditions, mitochondrial respiratory chain proteins produce $O_2^{\cdot-}$, which can be dismutated into hydrogen peroxide (H_2O_2) or react with nitric oxide to produce peroxynitrite. In addition, reaction of H_2O_2 with iron leads to hydroxyl radical formation via Fenton chemistry. During I/R injury, $O_2^{\cdot-}$ production in the vasculature is substantially increased (Wei et al., 1999) and is accompanied by endothelial cytotoxicity (for review see Li and Shah, 2004). However, the molecular mechanisms by which ROS lead to organ damage are poorly understood.

In pathological conditions, cell death is facilitated by an elevation in intracellular calcium ($[Ca^{2+}]_i$; Hajnoczky et al., 2003; Orrenius et al., 2003) via inositol 1,4,5-trisphosphate ($InsP_3$). $InsP_3$ is a second messenger produced by the hydrolysis of phosphatidylinositol-4,5-bisphosphate by PLC. $InsP_3$ receptor ($InsP_3R$)–mediated $[Ca^{2+}]_i$ changes are associated with a rapid, transient Ca^{2+} release from Ca^{2+} stores in the ER followed by Ca^{2+} entry through slow-activating plasma membrane store-operated channels (Putney and Bird, 1993; Parekh and Penner, 1997; Berridge et al., 1998). $InsP_3$ $[Ca^{2+}]_i$ signals control a wide range of cellular functions, including cell proliferation and apoptosis (Berridge et al., 2000; Orrenius et al., 2003). Apoptosis is reduced in cells lacking all three $InsP_3R$ isoforms (DT40 avian B cells) and after selective suppression of $InsP_3R$-3 (Jayaraman and Marks, 1997; Sugawara et al., 1997), indicating the important role of $InsP_3$ in cell death mechanisms (Pan et al., 2001). Alterations in $[Ca^{2+}]_i$ after oxidative stress facilitate

Correspondence to Muniswamy Madesh: madeshm@mail.med.upenn.edu

Abbreviations used in this paper: 2-APB, 2-aminoethoxydiphenyl borate; BAPTA, 1,2-bis(2-aminophenoxy)ethane-*N,N,N′,N′*-tetracetate; $[Ca^{2+}]_i$, intracellular calcium; $\Delta\Psi_m$, mitochondrial membrane potential; DCF, dichlorofluorescein; DPI, diphenyleneiodonium; ECM, extracellular medium; GPCR, G protein–coupled receptor; $InsP_3$, inositol 1,4,5-trisphosphate; $InsP_3R$, $InsP_3$ receptor; I/R, ischemia/reperfusion; KO, knockout; LPS, lipopolysaccharide; MPTP, mitochondrial permeability transition pore; PI, propidium iodide; PMVEC, pulmonary microvascular endothelial cell; ROS, reactive oxygen species; SOD, superoxide dismutase; t-BuOOH, tert-butyl hydroperoxide; Tg, thapsigargin; TKO, triple KO; TMRE, tetramethylrhodamine, ethyl ester, perchlorate.

The online version of this article contains supplemental material.

The Journal of Cell Biology, Vol. 170, No. 7, September 26, 2005 1079–1090
http://www.jcb.org/cgi/doi/10.1083/jcb.200505022

activation of the mitochondrial permeability transition pore (MPTP), which releases cytochrome *c* from the mitochondrial intermembrane space, leading to mitochondrial membrane potential ($\Delta\Psi_m$) loss, assembly of the apoptosome, and activation of downstream caspases (Crompton, 1999). Recent evidence suggested that cytochrome *c* transiently released from mitochondria interacts with $InsP_3R$ and amplifies Ca^{2+}-mediated apoptosis (Boehning et al., 2003).

Endothelial cells subjected to oxidative stress undergo apoptosis (Warren et al., 2000). Although there is evidence that perturbations of cellular Ca^{2+} homeostasis (including $[Ca^{2+}]_i$ elevation, ER Ca^{2+} depletion, and mitochondrial Ca^{2+} increases) occur, the mechanisms by which oxidative stress mediates endothelial apoptosis remain unclear. Events in the early stages of stress signaling include the mobilization of $[Ca^{2+}]_i$ (Patterson et al., 2004), the generation of ROS, and the formation of lipid peroxides. However, it is unclear whether radical formation is a consequence of Ca^{2+} mobilization or a parallel event in early stress signaling. The proximity between mitochondria and the ER facilitates a higher Ca^{2+} exposure in mitochondria relative to the cytosol when released from the ER (Rizzuto et al., 1998). During pathological situations, excess ER-released Ca^{2+} may be detrimental to mitochondrial function and may trigger mitochondrial fragmentation and apoptosis. Previously, Bcl-2 family proteins have been implicated in apoptosis by affecting cellular Ca^{2+} homeostasis (Pinton et al., 2000; Pan et al., 2001; Li et al., 2002). A recent study reported that a functional interaction of Bcl-2 with $InsP_3R$ attenuated $InsP_3R$ activation, which in turn controlled $InsP_3$-evoked Ca^{2+} release (Chen et al., 2004), in contrast to our findings that Bcl-X_L activates $InsP_3R$ (White et al., 2005). In addition, ER-localized Bax and Bak can either interfere with ER Ca^{2+} homeostasis or initiate apoptosis by activating caspase 12 (Zong et al., 2003).

We previously reported that cells exposed to $O_2^{\cdot-}$ induced a rapid and large cytochrome *c* release (Madesh and Hajnoczky, 2001). We now provide evidence that $O_2^{\cdot-}$ evokes a large, transient $[Ca^{2+}]_i$ pool release from the ER, causing mitochondrial Ca^{2+} elevation and rapid depolarization. Remarkably, the observed $InsP_3$-linked mitochondrial phase of apoptosis was specific to $O_2^{\cdot-}$ and not other oxidant species. The $O_2^{\cdot-}$-induced mitochondrial depolarization and downstream apoptotic cascades are independent of mitochondrial ROS production. Overall, this evidence provides a mechanism by which $O_2^{\cdot-}$ is a key signaling molecule that coordinates multiple processes that lead to mitochondrial apoptotic events and endothelial dysfunction.

Results

Lipopolysaccharide (LPS)-stimulated macrophages evoke Ca^{2+} transients in endothelial cells

Activated macrophages are known to generate ROS and may be involved in organ damage during I/R (Droge, 2002). To test the significance of the selective role of macrophage-derived ROS during pathophysiological conditions, LPS-stimulated murine macrophages were used as a $O_2^{\cdot-}$-generating source. We determined whether $O_2^{\cdot-}$ released from macrophages could evoke Ca^{2+} mobilization in two cell types, endothelial and HepG2 cells. ROS production in LPS-stimulated mouse macrophages was measured via H_2DCF-DA, which is a nonfluorescent dye that produces the fluorescent compound dichlorofluorescein (DCF) when oxidized by ROS. DCF fluorescence was measured in untreated macrophages and those stimulated with LPS (1 μg/ml) or a combination of LPS and the NADPH oxidase inhibitor diphenyleneiodonium (DPI; 30 μM). LPS stimulation was associated with a pronounced increase in DCF fluorescence that was attenuated by DPI treatment, suggesting that LPS stimulated ROS production through activation of oxidative burst reactions (Fig. 1 A). The activation of macrophage NADPH oxidase generates $O_2^{\cdot-}$ extracellularly without altering intracellular production of ROS by mitochondria (Lambeth, 2004). To elucidate whether a paracrine ROS signal can be transduced to adjacent cells in pathological conditions, LPS-stimulated macrophages were added onto pulmonary microvascular endothelial cells (PMVECs; Fig. 1 B) that had been previously loaded with the $[Ca^{2+}]_i$ indicator dye Fluo-4 (Fig. 1 C). Application of LPS-activated macrophages evoked a

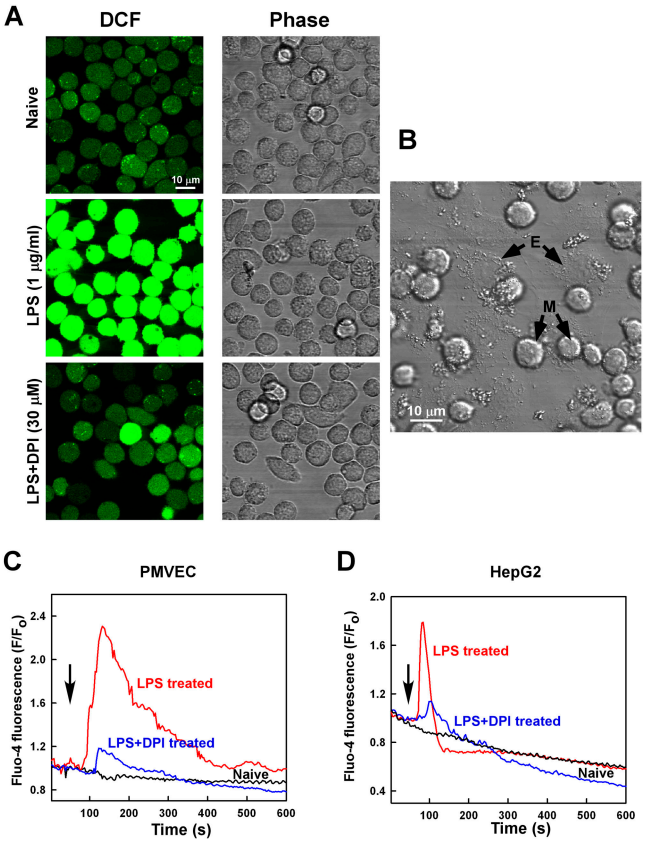

Figure 1. **Endothelial cell Ca^{2+} mobilization in response to activated macrophage-derived ROS.** (A) J774A.1 murine macrophages were activated by 1 μg/ml LPS for 3 h in the presence or absence of the flavoprotein inhibitor DPI for 1 h. Cells were incubated with 10 μM of the ROS-sensitive dye H_2DCF-DA and visualized using confocal microscopy. (B) Macrophages (M) were applied to PMVECs (E) to assess paracrine $O_2^{\cdot-}$ signaling. Ca^{2+} indicator Fluo-4/AM–loaded PMVECs (C; $n = 3$) and HepG2 cells (D) were exposed to nonactivated, LPS-treated, and LPS+DPI-treated macrophages Fluo-4 fluorescence change was recorded every 3 s for 10 min ($n = 2$). Ca^{2+} mobilization was measured as described in Materials and methods.

$[Ca^{2+}]_i$ rise in PMVECs that was attenuated by DPI pretreatment (Fig. 1 C). To exclude the contribution of autocrine extracellular ROS production, a similar experiment was performed using HepG2 parenchymal cells, as these cells generate minimal $O_2^{\cdot-}$ (Kikuchi et al., 2000). HepG2 cells displayed an $[Ca^{2+}]_i$ elevation after LPS-stimulated macrophage exposure, whereas no $[Ca^{2+}]_i$ transient was noted after application of non-stimulated macrophages (Fig. 1 D). In contrast, exposure of HepG2 cells to macrophages that had been stimulated by LPS plus DPI triggered only an extremely small $[Ca^{2+}]_i$ rise (Fig. 1 D). The oscillatory $[Ca^{2+}]_i$ transient pattern observed in individual HepG2 cells but not PMVECs is notable, indicating a potential difference in Ca^{2+} handling between cell types (unpublished data). Overall, this result suggests that $O_2^{\cdot-}$ is specifically required for elevation of $[Ca^{2+}]_i$ in endothelial cells.

$O_2^{\cdot-}$ evokes endothelial Ca^{2+} transients through $InsP_3$ signaling

To identify the mechanisms by which $O_2^{\cdot-}$ triggers $[Ca^{2+}]_i$ signals in PMVECs, we extended our studies to examine the effects of $O_2^{\cdot-}$ on basal $[Ca^{2+}]_i$. To exclude the possible contribution of other macrophage factors, the xanthine+xanthine oxidase (X+XO) system was used to generate $O_2^{\cdot-}$ externally. Cells exposed to $O_2^{\cdot-}$ demonstrated a rapid increase in $[Ca^{2+}]_i$ followed by a slightly delayed return to baseline (Fig. 2 A). Similarly, the physiological stimulus ATP generated a marked $[Ca^{2+}]_i$ transient (Fig. S1, available at http://www.jcb.org/cgi/content/full/jcb.200505022/DC1). The $O_2^{\cdot-}$-evoked $[Ca^{2+}]_i$ increase was abolished by pretreatment with the XO inhibitor allopurinol (1 mM; Fig. 2 B) or by a combination of the antioxidant superoxide dismutase (SOD; 2000 U/ml) and the anion channel blocker DIDS (100 μM; Fig. 2 C). Treatment with either xanthine or allopurinol did not alter basal $[Ca^{2+}]_i$ in control cells (unpublished data). These findings suggest that acute exposure of PMVECs to extracellular $O_2^{\cdot-}$ results in a rapid $[Ca^{2+}]_i$ rise. We next sought to determine the source of the elevated $[Ca^{2+}]_i$. Thapsigargin (Tg) inhibits the SERCA Ca^{2+}ATPase, causing Ca^{2+} depletion from the ER (Ma et al., 2000, 2001). Pretreatment with 2 μM Tg virtually abolished $O_2^{\cdot-}$-induced Ca^{2+} transients (Fig. 2 D). Conversely, removal of Ca^{2+} from the external medium was without effect on $[Ca^{2+}]_i$ (Fig. 2 E). Together, these results indicate that $O_2^{\cdot-}$ induces a release of Ca^{2+} from internal stores. ER Ca^{2+} stores in endothelial cells can be modulated by production of the second messenger $InsP_3$ by PLC and subsequent binding to receptors on the ER ($InsP_3R$). To characterize the release of Ca^{2+} from intracellular stores, PMVECs were pretreated for 10 min with either the PLC inhibitor U-73122 or its inactive analogue U-73343. U-73122, but not U-73343 (both 100 μM), inhibited the $O_2^{\cdot-}$-induced Ca^{2+} release (Fig. 2, F and G). This result suggests that the $O_2^{\cdot-}$-induced $[Ca^{2+}]_i$ transient was mediated by $InsP_3$. To further characterize $O_2^{\cdot-}$-induced Ca^{2+} release, cells were incubated with 2-aminoethoxydiphenyl borate (2-APB; 75 μM) before $O_2^{\cdot-}$ stimulation. 2-APB has widely been used as an inhibitor of $InsP_3$-sensitive Ca^{2+} release and store-operated Ca^{2+} channels in intact cells (Ma et al., 2001; Bootman et al., 2002). In agreement with our PLC data, $O_2^{\cdot-}$-induced Ca^{2+} transients were abolished in cells pretreated with 2-APB (Fig. 2, H and I). Thus, the $O_2^{\cdot-}$-induced $[Ca^{2+}]_i$ rise in PMVECs was due to the $InsP_3$-dependent release of Ca^{2+} from internal stores.

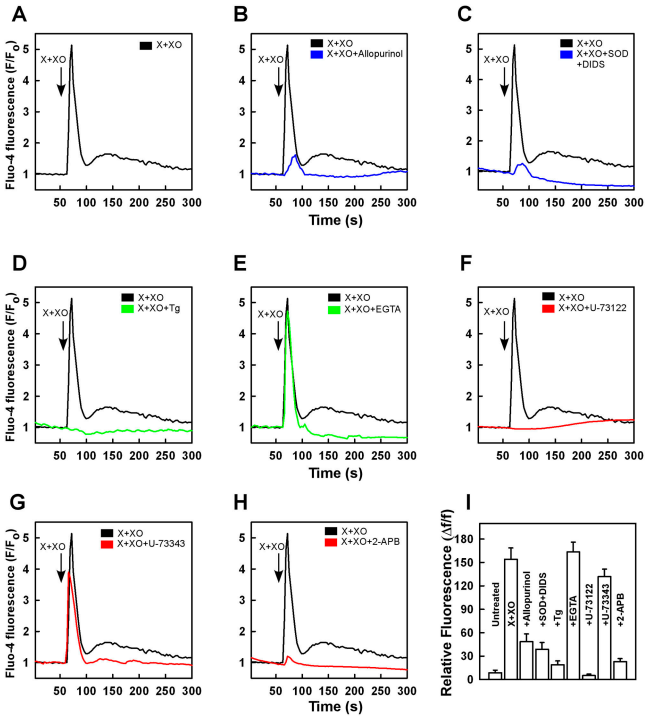

Figure 2. **Extracellular $O_2^{\cdot-}$ induces $[Ca^{2+}]_i$ mobilization through an $InsP_3$-dependent pathway.** (A) Fluo-4/AM–loaded PMVECs exposed to the $O_2^{\cdot-}$-generating system (100 μM X +5 mU/ml XO) display a Ca^{2+} transient (n = 15). (B and C) Inhibition of XO by 1 mM allopurinol and combination scavenge (2000 U/ml SOD) and entry inhibition (100 μM DIDS) attenuated Ca^{2+} mobilization (n = 3). Intracellular store depletion (2 μM Tg; D; n = 4) but not extracellular Ca^{2+} chelation (10 mM EGTA; E) prevented $O_2^{\cdot-}$-evoked $[Ca^{2+}]_i$ mobilization (n = 3). (F and G) The PLC inhibitor U-73122 (100 μM) abolishes the $[Ca^{2+}]_i$ rise, whereas the analogue U-73343 (100 μM) fails to inhibit the $O_2^{\cdot-}$ effect (n = 4). (H) Pretreatment with 75 μM of the $InsP_3R$ antagonist 2-APB eliminated the $O_2^{\cdot-}$ effect (n = 4). (I) Relative Fluo-4 fluorescence change was quantified. Data are means ± SEM.

$O_2^{\cdot-}$-triggered $[Ca^{2+}]_i$ release is abolished in $InsP_3R$ triple knockout (TKO) cells

To examine the specific role of $InsP_3R$ in the $O_2^{\cdot-}$-triggered $[Ca^{2+}]$ rise, the $InsP_3R$-deficient DT40 chicken B-lymphocyte cell line (DT40 $InsP_3R$ TKO) was used. Wild-type cells demonstrated a significant $[Ca^{2+}]_i$ increase after $O_2^{\cdot-}$ exposure. After $[Ca^{2+}]_i$ returned to basal levels, 2 μM Tg was added to the medium to induce a transient increase in $[Ca^{2+}]_i$ as a consequence of passive depletion of endogenous stores upon ER Ca^{2+}/Mg^{2+}-ATPase blockade (Fig. 3, A and B). Similar to PMVECs, pretreatment with 2 μM Tg eliminated the $O_2^{\cdot-}$-induced Ca^{2+} transients in wild-type DT40 cells (unpublished data). In contrast, addition of a $O_2^{\cdot-}$ pulse failed to elicit Ca^{2+} release from intracellular stores in DT40 $InsP_3R$ TKO cells, whereas subsequent addition of 2 μM Tg triggered a complete depletion of Ca^{2+} stores (Fig. 3, A and B). These data suggest that Ca^{2+} release through the $InsP_3R$ underlies the $O_2^{\cdot-}$-evoked rise of $[Ca^{2+}]_i$. To confirm that DT40 $InsP_3R$ TKO cells retain the machinery necessary for the $O_2^{\cdot-}$-mediated $[Ca^{2+}]_i$ tran-

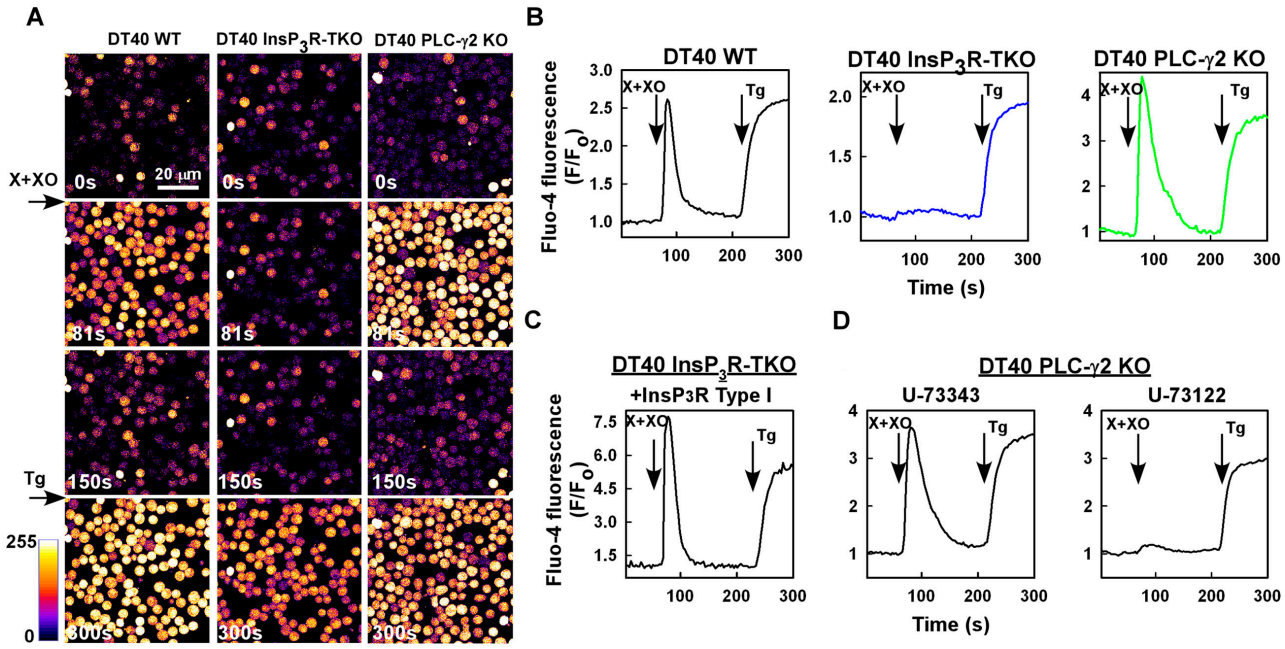

Figure 3. **Elimination of $O_2^{\cdot-}$-evoked $[Ca^{2+}]_i$ mobilization in $InsP_3R$ TKO cells.** (A) Fluo-4/AM–loaded DT40 chicken B lymphocytes display a normal Ca^{2+} response to extracellular $O_2^{\cdot-}$ (100 μM X + 5 mU/ml XO; $n = 7$). In DT40 InsP3R TKO cells, $O_2^{\cdot-}$ failed to elicit $[Ca^{2+}]_i$ rise, whereas the subsequent addition of 2 μM Tg caused a large store depletion ($n = 3$). $O_2^{\cdot-}$-evoked Ca^{2+} mobilization is not dependent on PLC-γ2–mediated $InsP_3$ production ($n = 3$). (B) Quantitation of $[Ca^{2+}]_i$ transient in wild-type DT40, TKO, and PLC-γ2 KO cells. (C) Measurement of $[Ca^{2+}]_i$ transient in DT40 $InsP_3R$ TKOs after re-expression of $InsP_3R$ Type I ($n = 4$). 38 out of 369 cells displayed $[Ca^{2+}]_i$ transient after $O_2^{\cdot-}$ exposure, as demonstrated by the single cell tracing. (D) PLC-γ2 KO of DT40 cells pretreated with U-73122 but not U-73343 attenuated Ca^{2+} release from stores after exposure to $O_2^{\cdot-}$ ($n = 3$).

sient, we transfected the rat $InsP_3R$ type I into TKO cells. This procedure restored the responsiveness of TKO cells to $O_2^{\cdot-}$ (Fig. 3 C). This result indicates that in TKO cells, a $O_2^{\cdot-}$-mediated signal activates $InsP_3R$ type I and causes Ca^{2+} release from ER store.

In PMVECs, inhibition of PLC with U-73122 prevented the rise of $[Ca^{2+}]_i$ induced by exposure to $O_2^{\cdot-}$. We therefore further investigated the role of PLC in $O_2^{\cdot-}$-triggered Ca^{2+} mobilization using PLC-γ2–deficient DT40 cells. $O_2^{\cdot-}$ exposure triggered a substantial rise of $[Ca^{2+}]_i$ in PLC-γ2–deficient DT40 cells (Fig. 3, A and B). In wild-type DT40 cells, B cell receptor agonist IgM (2 μg/ml) induced a series of rapid $[Ca^{2+}]_i$ oscillations representing $[Ca^{2+}]_i$ release and reuptake. In contrast, anti-IgM failed to elicit Ca^{2+} mobilization in both $InsP_3R$ TKO and PLC-γ2 knockout (KO) cells (unpublished data). These data indicate that the nonreceptor tyrosine kinase–linked cascade, to which PLC-γ2 is coupled, is dispensable for the $O_2^{\cdot-}$-triggered $[Ca^{2+}]_i$ rise. In agreement with our findings, G protein–coupled receptor (GPCR)–mediated Ca^{2+} oscillations were previously abolished by U-73122, which inhibits all PLC-β isoforms (Zeng et al., 2003). To further understand the role of $InsP_3$, PLC-γ2 KO cells were pretreated with either PLC inhibitor U-73122 or U-73343 as described in Fig. 2 (F and G). U-73122, but not U-73433, attenuated the $O_2^{\cdot-}$-evoked $[Ca^{2+}]_i$ rise (Fig. 3 D). To ensure that the $O_2^{\cdot-}$ elicits $InsP_3$ accumulation, $InsP_3$ was assessed in wild-type DT40, DT40 $InsP_3R$ TKO, and DT40 PLC-γ2 KO cells. Direct measurement of $InsP_3$ production indicated that $O_2^{\cdot-}$ markedly activated $InsP_3$ formation in wild-type DT40, DT40 $InsP_3R$ TKO, and DT40 PLC-γ2 KO cells. In contrast, pretreatment of DT40 PLC-γ2 KO cells with U-73122 significantly attenuated this response (Fig. S2 A, available at http://www.jcb.org/cgi/content/full/jcb.200505022/DC1). Similarly, PMVECs exposed to $O_2^{\cdot-}$ exhibited markedly greater $InsP_3$ production than the physiological stimulus ATP (Fig. S2 B). Collectively, these findings suggest that extracellular $O_2^{\cdot-}$ causes Ca^{2+} release via a PLC-mediated increase in $InsP_3$.

$O_2^{\cdot-}$ mediates coupling of $[Ca^{2+}]_i$ elevation and mitochondrial uptake

It is believed that agonist-induced $[Ca^{2+}]_i$ rise can be buffered by mitochondria (Bernardi and Petronilli, 1996). To determine if the $O_2^{\cdot-}$-triggered $[Ca^{2+}]_i$ spike is delivered to mitochondria, rhod-2– (mitochondrial Ca^{2+} indicator) and Fluo-4–loaded PMVECs were subjected to $O_2^{\cdot-}$. Exposure of PMVECs to $O_2^{\cdot-}$ induced an $[Ca^{2+}]_i$ increase as evidenced by an increase in Fluo-4 fluorescence, as shown earlier (Fig. 2 A), followed by an elevation of mitochondrial Ca^{2+} fluorescence (Fig. 4, A and B). Similarly, ATP induced a $[Ca^{2+}]_i$ rise followed by mitochondrial $[Ca^{2+}]$ elevation (Fig. 4, C and D). These results indicate Ca^{2+} signal propagation from the cytosol to the mitochondria in both physiological (purinergic receptor agonist) and pathological conditions (oxidative stress). Notably, $O_2^{\cdot-}$-evoked mitochondrial Ca^{2+} elevation was increased and sustained compared with the transient pattern observed in response to ATP. These results suggest that $O_2^{\cdot-}$-induced intracellular pool Ca^{2+} release evokes elevated mitochondrial Ca^{2+} uptake during oxidative stress.

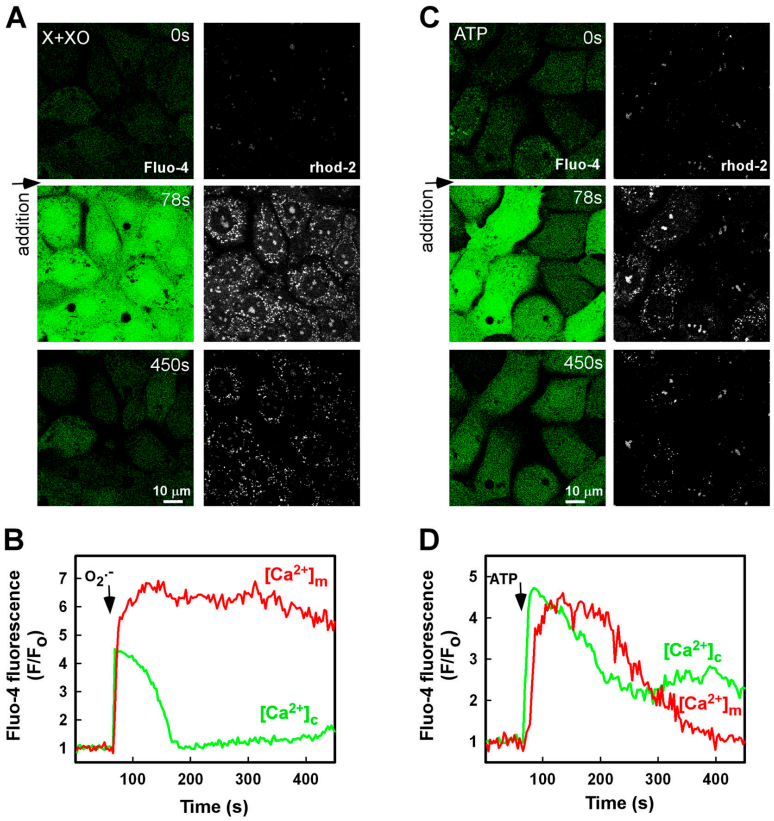

Figure 4. **Coupling of $O_2^{\cdot-}$-evoked cytosolic Ca^{2+} elevation and mitochondrial Ca^{2+} signaling in endothelial cells.** Simultaneous imaging of $O_2^{\cdot-}$ (100 μM X+ 5 mU/ml XO) or ATP (100 μM) induced changes in cytosolic and mitochondrial Ca^{2+} using Fluo-4/AM and compartmentalized rhod-2/AM. (A and C, left) Images show the $[Ca^{2+}]_i$ response to addition of $O_2^{\cdot-}$ and ATP. (A and C, right) Confocal images of endothelial cells loaded with the mitochondrial Ca^{2+} indicator rhod-2 display Ca^{2+} accumulation ($n = 4$). (B and D) Synchronized measurements of $O_2^{\cdot-}$- or ATP-induced changes in cytosolic and mitochondrial Ca^{2+}. $O_2^{\cdot-}$, but not ATP, triggered cytosolic Ca^{2+} mobilization and sustained mitochondrial Ca^{2+} elevation. The experimental data indicate that cytosolic Ca^{2+} elevation precedes mitochondrial Ca^{2+} uptake.

$O_2^{\cdot-}$-induced Ca^{2+} transients evoke rapid mitochondrial depolarization

Reversible depolarization of $\Delta\Psi_m$ occurs as a consequence of electrogenic uptake of Ca^{2+} by mitochondria in response to transient $[Ca^{2+}]_i$ (Duchen, 1992). However, ROS may also promote MPTP opening (Huser et al., 1998). Because mitochondrial Ca^{2+} elevation is a common pathway in both normal physiological and pathological stimuli, we examined whether the observed mitochondrial Ca^{2+} uptake after $O_2^{\cdot-}$ exposure is associated with mitochondrial depolarization. Simultaneous fluorescence measurements of $[Ca^{2+}]_i$ and $\Delta\Psi_m$ were conducted in PMVECs during $O_2^{\cdot-}$ exposure (Fig. 5, A and B). In response to ATP, an $[Ca^{2+}]_i$ rise was observed similar to that in cells after $O_2^{\cdot-}$ exposure. However, in contrast to $O_2^{\cdot-}$, PMVECs exposed to ATP exhibited only a nominal change in $\Delta\Psi_m$ (Fig. 5 C), possibly due to transient Ca^{2+} uptake (Fig. 4, B and D). Application of $O_2^{\cdot-}$ evoked a rapid and transient rise in $[Ca^{2+}]_i$ that preceded a decrease in tetramethylrhodamine, ethyl ester, perchlorate (TMRE) fluorescence, indicating that mitochondrial depolarization is associated with the onset of the $[Ca^{2+}]_i$ rise (Fig. 5 B). Because $O_2^{\cdot-}$ is rapidly dismutated into H_2O_2, we sought to determine which oxidants are involved in the observed $\Delta\Psi_m$ loss. Cells incubated with H_2O_2 (1 mM) displayed no rapid $[Ca^{2+}]_i$ transient. Rather, H_2O_2 induced a slight increase in $[Ca^{2+}]_i$ (Fig. 5 D) and a delayed loss of $\Delta\Psi_m$. Tg pretreatment did not affect the H_2O_2-facilitated slow $[Ca^{2+}]_i$ rise (unpublished data). These findings suggest that H_2O_2 may not affect the intracellular store, but instead facilitates Ca^{2+} entry from the extracellular milieu independent of mitochondrial depolarization. Oxidized phospholipid byproducts are involved in cell death during oxidative stress (Ran et al., 2004). However, the lipid-oxidizing agent t-butyl hydroperoxide (t-BuOOH; 200 μM) did not evoke either an $[Ca^{2+}]_i$ rise or $\Delta\Psi_m$ loss (Fig. 5 E). This finding suggests the selective role of $O_2^{\cdot-}$, and not other oxidants, in eliciting an $[Ca^{2+}]_i$ rise and mitochondrial depolarization.

Extracellular $O_2^{\cdot-}$-mediated signaling functions independent of mitochondrially derived ROS

Evidence indicates that external ROS may evoke mitochondrial $O_2^{\cdot-}$ production (Zorov et al., 2000; Aon et al., 2003). Because the $O_2^{\cdot-}$-evoked $[Ca^{2+}]_i$ rise is a prerequisite for $\Delta\Psi_m$ loss, we aimed to exclude the involvement of intracellular ROS production by mitochondrial electron transport proteins in $\Delta\Psi_m$ loss. Antimycin A inhibits the normal electron flow through complex III, but triggers $O_2^{\cdot-}$ production through the accumulation of ubisemiquinone. Antimycin A triggered an immediate $\Delta\Psi_m$ loss without an apparent change in $[Ca^{2+}]_i$ (Fig. 6 A). Rotenone inhibits electron transfer from complex I (NADH dehydrogenase) to ubiquinone and diminishes $O_2^{\cdot-}$ production from complex III (Turrens et al., 1985). In contrast to antimycin A, rotenone affected neither $[Ca^{2+}]_i$ nor $\Delta\Psi_m$. However, subsequent addition of $O_2^{\cdot-}$ triggered an $[Ca^{2+}]_i$ rise followed by $\Delta\Psi_m$ loss (Fig. 6 B). Oligomycin, which inhibits the mitochondrial F_oF_1-ATPase by binding to ATP synthase, was used to exclude possible mitochondrial ATP-dependent ROS production. Treatment with oligomycin failed to trigger either $[Ca^{2+}]_i$ mobilization or $\Delta\Psi_m$ loss. Subsequent addition of $O_2^{\cdot-}$ established both events

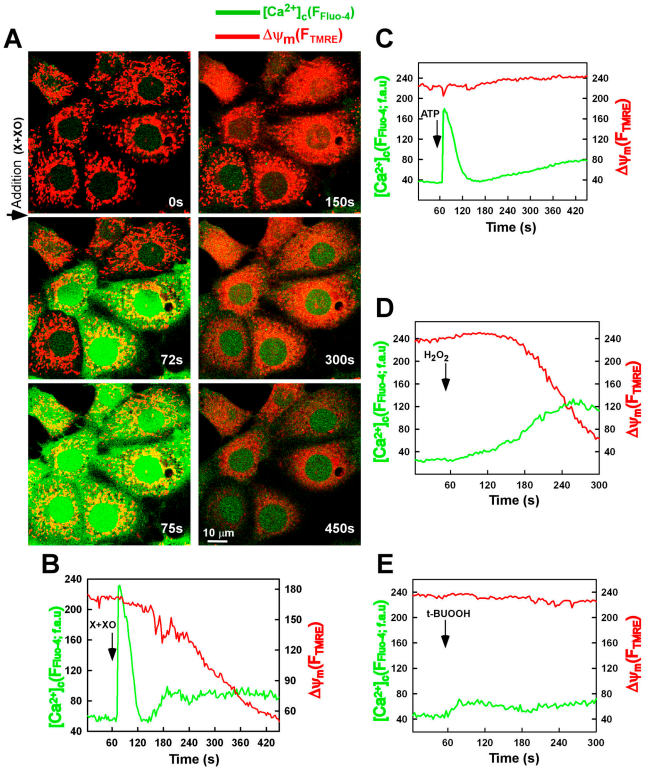

Figure 5. **Selective $O_2^{\cdot-}$ induction of Ca^{2+} signaling evokes mitochondrial depolarization.** (A) PMVECs loaded with Fluo-4/AM (30 min) and stained with TMRE (15 min) were exposed to $O_2^{\cdot-}$ as indicated ($n = 8$). (B) Relative brightness of Fluo-4 fluorescence and punctate–diffuse index of TMRE was calculated and plotted over time. (C) Change in $[Ca^{2+}]_i$ and $\Delta\Psi_m$ in response to 100 μM ATP ($n = 3$). $[Ca^{2+}]_i$ level and mitochondrial $\Delta\Psi_m$ were recorded in response to 1 mM H_2O_2 (D; $n = 4$) and 200 μM t-BuOOH (E; $n = 4$).

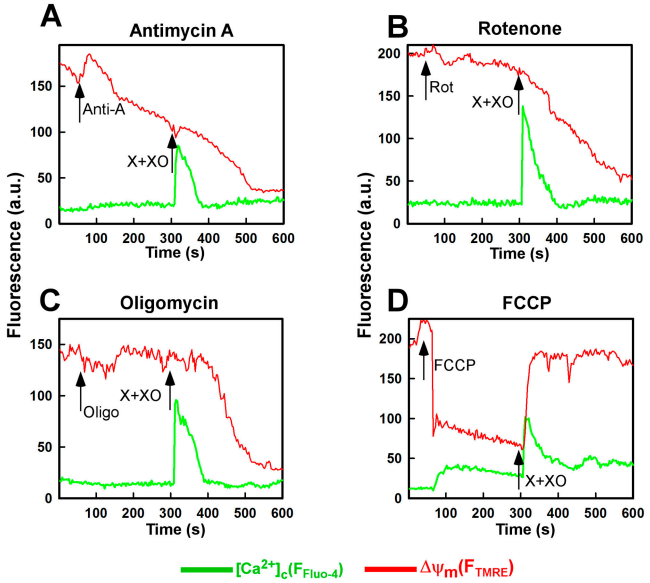

Figure 6. **Contribution of mitochondrially derived ROS on the Ca^{2+} transient and mitochondrial depolarization.** (A) 20 μM antimycin A immediately induced $\Delta\Psi_m$ without an apparent elevation of $[Ca^{2+}]_i$. $\Delta\Psi_m$ was further exaggerated by subsequent application of $O_2^{\cdot-}$ in Fluo-4/AM– and TMRE-loaded PMVECs ($n = 4$). (B) 20 μM rotenone failed to demonstrate either a Ca^{2+} transient or mitochondrial depolarization. Subsequent addition of $O_2^{\cdot-}$ facilitated $[Ca^{2+}]_i$ mobilization followed by $\Delta\Psi_m$ ($n = 3$). (C) 10 μg/ml oligomycin did not affect either $[Ca^{2+}]_i$ levels or $\Delta\Psi_m$, and successive addition of $O_2^{\cdot-}$ facilitated $[Ca^{2+}]_i$ pool depletion and $\Delta\Psi_m$ ($n = 3$). (D) Exposure to 3 μM of the mitochondrial uncoupler FCCP before addition of $O_2^{\cdot-}$ caused a rapid $\Delta\Psi_m$ dissipation and $[Ca^{2+}]_i$ elevation that was reestablished by $O_2^{\cdot-}$ ($n = 4$).

(Fig. 6 C). This result indicates that complex III is the major site of mitochondrial ROS production during oxidative stress. It has been reported that mitochondrial Ca^{2+} uptake requires an intact $\Delta\Psi_m$ and that dissipation by a mitochondrial uncoupler abolishes mitochondrial Ca^{2+} uptake and delays $[Ca^{2+}]_i$ clearance (Boitier et al., 1999). Close examination of PMVECs exposed to the mitochondrial uncoupler FCCP revealed that a rapid $\Delta\Psi_m$ loss was associated with $[Ca^{2+}]_i$ elevation (Fig. 6 D). This $[Ca^{2+}]_i$ rise most likely reflects Ca^{2+} release from the mitochondria as a consequence of mitochondrial depolarization. Surprisingly, subsequent application of $O_2^{\cdot-}$ evoked a transient rise in cytosolic Fluo-4 fluorescence followed by a rapid recovery of $\Delta\Psi_m$. The $\Delta\Psi_m$ recovered after $O_2^{\cdot-}$ treatment is almost identical to the initial potential observed before FCCP addition. Collectively, these results suggest that the mitochondrial ROS-evoked $\Delta\Psi_m$ loss is independent of $InsP_3R$-linked $\Delta\Psi_m$ changes by $O_2^{\cdot-}$.

Ca^{2+} buffering protects against $O_2^{\cdot-}$-triggered mitochondrial depolarization

To assess whether the $O_2^{\cdot-}$-induced rise of $[Ca^{2+}]_i$ is required for the $O_2^{\cdot-}$-evoked $\Delta\Psi_m$ loss, PMVECs were loaded with the Ca^{2+} chelator 1,2-bis(2-aminophenoxy)ethane-*N*,*N*,*N*′,*N*′-tetraacetate (BAPTA) by incubation with the permeant acetoxymethyl ester (25 μM for 30 min) before application of the $O_2^{\cdot-}$. BAPTA loading significantly inhibited $O_2^{\cdot-}$-induced $\Delta\Psi_m$ loss (Fig. 7, A and B). In contrast, the H_2O_2-induced $\Delta\Psi_m$ loss was unaffected by pretreatment with BAPTA (Fig. 7 C). These experimental data provide evidence that $\Delta\Psi_m$ loss induced specifically by $O_2^{\cdot-}$ requires a rise of $[Ca^{2+}]_i$. Other oxidants such as H_2O_2 are deleterious to mitochondrial function but appear to affect $\Delta\Psi_m$ through a Ca^{2+}-independent pathway.

$O_2^{\cdot-}$-mediated signaling triggers caspase activation

Caspase cysteine proteases augment mitochondrial dysfunction by both activating proapoptotic Bcl-2 family proteins such as Bax, Bak, and Bid and inactivating antiapoptotic proteins such as Bcl-2 (Wei et al., 2001). To determine the dose and time course of receptor-mediated and mitochondrially dependent caspase activation in PMVECs after oxidant exposure, cytosolic extracts were collected after treatment with $O_2^{\cdot-}$, H_2O_2, and t-BuOOH. Remarkably, when cells were exposed to $O_2^{\cdot-}$, robust caspase-3 activity was observed in a dose-dependent manner (Fig. 8, A and D). Interestingly, even a low dose (1 mU X+XO) was able to induce caspase-3 activity, indicating that $O_2^{\cdot-}$ may activate downstream caspases through a mitochondrially dependent pathway. Similarly, prominent caspase-9 activity was observed after $O_2^{\cdot-}$ treatment (Fig. 8, C and F). H_2O_2 elicited some caspase-3 and -9 activity, but at a level several-fold less than $O_2^{\cdot-}$. In contrast, t-BuOOH did not activate either

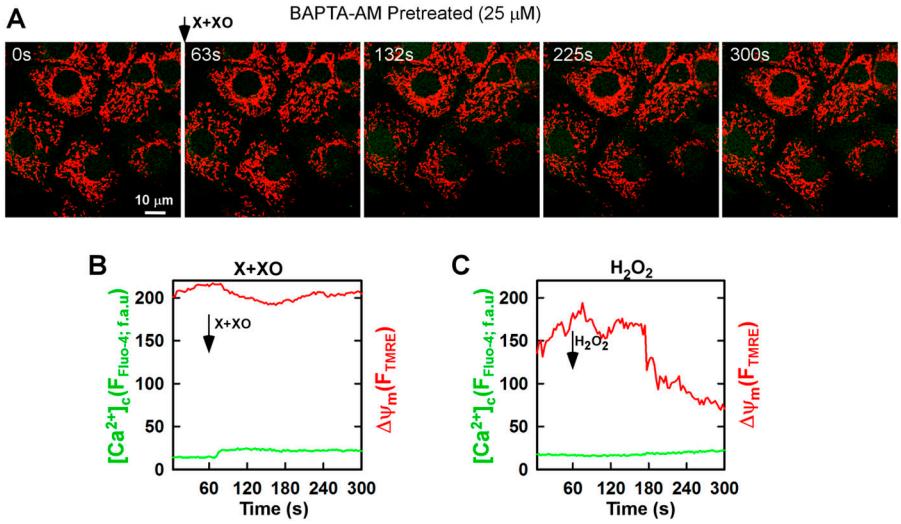

Figure 7. **Buffering of $O_2^{\cdot-}$-evoked $[Ca^{2+}]_i$ elevation with BAPTA prevents Ca^{2+}-induced $\Delta\Psi_m$ in PMVECs.** (A and B) $O_2^{\cdot-}$-induced $[Ca^{2+}]_i$ elevation and $\Delta\Psi_m$ was prevented by pretreatment of cells with 25 μM of the membrane-permeable Ca^{2+} chelator (BAPTA-AM; $n = 4$). (C) Chelation of intracellular Ca^{2+} using BAPTA failed to attenuate H_2O_2-induced $\Delta\Psi_m$ ($n = 4$).

caspase-3 or -9. During apoptotic conditions, caspase-8 can activate caspase-3 directly through an extrinsic pathway. As shown in Fig. 8 (B and E), treatment of PMVECs with $O_2^{\cdot-}$ induced caspase-8 activity that was sevenfold higher than control and other oxidants. Inhibition of $\Delta\Psi_m$ loss by $[Ca^{2+}]_i$ buffering prevented caspase-3 and -9 activation (Fig. 8, D and F). Collectively, these results provide evidence that $O_2^{\cdot-}$ activates both extrinsic and intrinsic caspase pathways.

$O_2^{\cdot-}$-evoked $[Ca^{2+}]i$ overload executes the cell death machinery

Our results reveal that $O_2^{\cdot-}$ stimulates $[Ca^{2+}]_i$ mobilization that triggers subsequent mitochondrial events, leading to caspase activation in PMVECs. To directly demonstrate that $O_2^{\cdot-}$ induces apoptosis, we treated PMVECs with various oxidants at different doses, and then stained them for the early apoptotic marker annexin V and the late stage apoptotic (or necrotic) marker propidium iodide (PI). Cells treated with $O_2^{\cdot-}$ for 5 h displayed positive annexin V staining with no detectable PI labeling, indicating cells in the early stages of apoptosis (Fig. 9 A). Strikingly, cells exposed to a high concentration of $O_2^{\cdot-}$ demonstrated a dose-dependent elevation of both apoptotic and necrotic cell death as displayed in Fig. 9 B. Cells treated with 500 μM H_2O_2 also revealed an apoptotic phenotype, although at a lower level than observed in response to $O_2^{\cdot-}$. In contrast, t-BuOOH (200 μM) treatment primarily led to necrosis, as evidenced by positive annexin V and PI staining. Control conditions resulted in nominal levels of apoptotic- or necrotic-positive cells. Previously, our results provided evidence that buffering of $O_2^{\cdot-}$ evoked $[Ca^{2+}]_i$ rise by BAPTA-AM and markedly prevented PMVEC $\Delta\Psi_m$ loss. Therefore, we tested whether $[Ca^{2+}]_i$ buffering inhibits $O_2^{\cdot-}$-induced apoptosis. BAPTA-AM pretreatment (25 μM) attenuated apoptosis in PMVECs (Fig. 9 C), providing evidence that $O_2^{\cdot-}$-induced $[Ca^{2+}]_i$ elevation is essential for mitochondrially dependent apoptosis. Conversely, BAPTA-AM treatment was ineffective 20 min after application of the $O_2^{\cdot-}$ (unpublished data). DT40 B-cells lacking all forms of $InsP_3R$ display reduced apoptotic cell death in response to anti-IgM

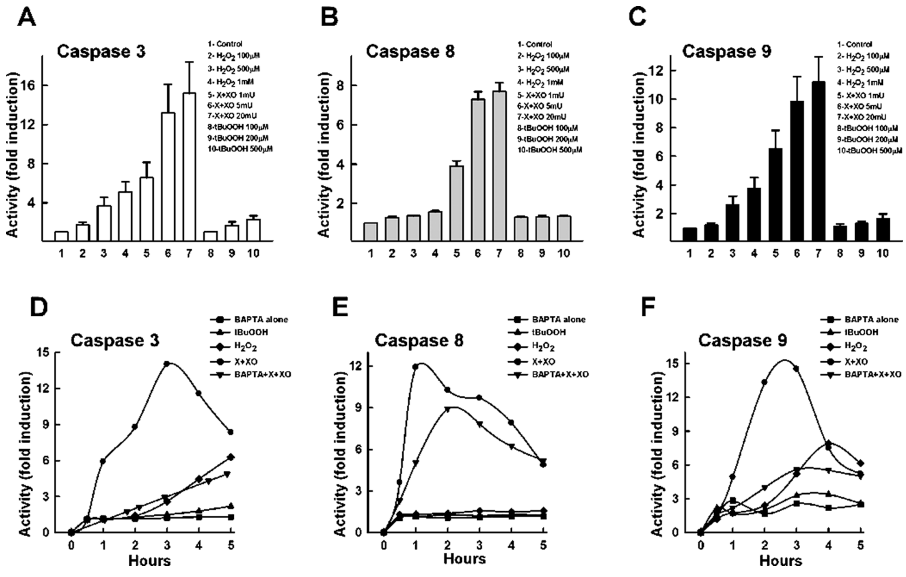

Figure 8. **$O_2^{\cdot-}$-dependent activation of caspases in PMVECs.** Cells were exposed to various concentrations of $O_2^{\cdot-}$, H_2O_2, and t-BuOOH. After 3 h of treatment, lysates were assessed for caspase-3 ($n = 3$; A), -8 ($n = 3$; B), and -9 ($n = 3$; C) activity. Time-dependent experiments were also performed for caspase-3 ($n = 3$; D), -8 ($n = 3$; E), and -9 ($n = 3$; F). Pretreatment with 25 μM BAPTA-AM for 30 min attenuated caspase-3, -8, and -9 ($n = 3$) activation in response to $O_2^{\cdot-}$ as indicated in D, E, and F. Control cells were treated with 25 μM BAPTA-AM alone. Data are means ± SEM.

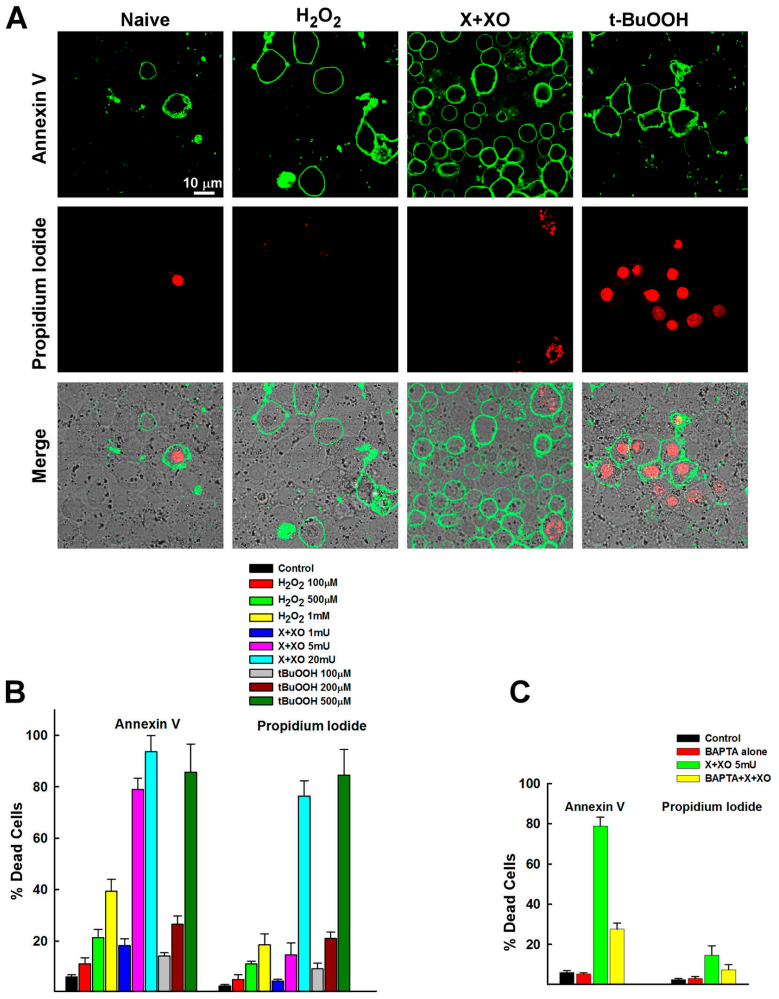

Figure 9. **$O_2^{\cdot-}$ signaling selectively evokes apoptosis in PMVECs.** After a 5-h exposure to $O_2^{\cdot-}$, H_2O_2, or t-BuOOH, cells were labeled with annexin V Alexa Fluor-488 conjugate and PI for 15 min. (A) Cells exposed to $O_2^{\cdot-}$ (X+XO; 5 mU/ml; $n = 3$) demonstrated positive annexin V staining, indicating early apoptosis. H_2O_2 (500 μM; $n = 3$) treatment demonstrated considerably less positive annexin V staining. Cells treated with 200 μM t-BuOOH ($n = 3$) stained positive for both annexin V and PI, indicating membrane permeabilization and necrotic cell death. (B) Quantitation of annexin V– and PI-positive cells after exposure to ROS. (C) $[Ca^{2+}]_i$ chelation (BAPTA-AM; 25 μM) attenuated $O_2^{\cdot-}$-induced cell death ($n = 3$). Data are means ± SEM.

(Sugawara et al., 1997). Because $O_2^{\cdot-}$-induced $[Ca^{2+}]_i$ elevation is ablated in DT40 $InsP_3R$ TKO cells, we next investigated apoptosis in DT40 cells. DT40 $InsP_3R$ TKO cells, but not wild-type cells, display increased resistance to apoptosis after $O_2^{\cdot-}$ application (Fig. S3, available at http://www.jcb.org/cgi/content/full/jcb.200505022/DC1). These results suggest that $O_2^{\cdot-}$ selectively alters ER Ca^{2+} homeostasis resulting in caspase activation, which in turn leads to apoptosis.

Discussion

The mechanisms that contribute to apoptosis during I/R injury remain unclear, but it is generally believed that the release and/or activation of various bioactive molecules, such as ROS (Zhao, 2004) and inflammatory cytokines (Haimovitz-Friedman et al., 1997), are responsible for cell death. During these conditions, xanthine (Malis and Bonventre, 1986) and NADPH oxidases play a key role in $O_2^{\cdot-}$ production (Wei et al., 1999) and trigger pathological signaling. Reperfusion of ischemic cells generates oxidative stress and alters mitochondrial function (Hausenloy et al., 2004). Coordination of mitochondrial function during injury is an essential component of cell physiology and survival, yet little is known about the factors that contribute to cell death during oxidative stress. This study demonstrates that $O_2^{\cdot-}$ facilitates a transient $[Ca^{2+}]_i$ elevation followed by mitochondrial Ca^{2+} uptake and depolarization that ultimately induces apoptotic cascades in endothelial cells.

Macrophage activation by endotoxin elicits $O_2^{\cdot-}$ generation via NADPH oxidase and autocrine production of ROS (Johnston et al., 1978). However, whether released $O_2^{\cdot-}$ has a potential paracrine signaling role in nearby cells is unknown. This study provides direct evidence that activated macrophages initiate an ROS-induced $[Ca^{2+}]_i$ elevation in adjacent cells. In comparison to the macrophage data, the observed $[Ca^{2+}]_i$ transient using the X+XO was larger and less sustained. The enzymatic X+XO system generates only $O_2^{\cdot-}$, whereas activated macrophages may release other factors that could alter the amplitude of $[Ca^{2+}]_i$ in PMVECs. In addition, xanthine oxidase has been shown to interact with the vascular endothelium during inflammatory conditions (Houston et al., 1999). Because of the short half-life of the $O_2^{\cdot-}$ radical, close association between endothelial cells and the $O_2^{\cdot-}$ source may facilitate a greater response. A single pulse of $O_2^{\cdot-}$ evoked an $[Ca^{2+}]_i$ rise in PMVECs that caused $\Delta\Psi_m$ loss. These results suggest a potential mechanism by which macrophage-mediated oxidative stress perpetuates endothelial dysfunction. This $O_2^{\cdot-}$-mediated response has several features. The $[Ca^{2+}]_i$ signals were observed in adherent PMVECs, HepG2, and DT40 suspension cell types, indicating a

common mechanism in the cellular response to $O_2^{\cdot-}$. The $O_2^{\cdot-}$-evoked $[Ca^{2+}]_i$ signal was prevented by the combination of SOD and the anion channel blocker DIDS. The $O_2^{\cdot-}$-induced transient rise of $[Ca^{2+}]_i$ was propagated to mitochondria, where a sustained Ca^{2+} elevation was observed. In contrast, the $[Ca^{2+}]_i$ response to the physiological stimulus ATP triggered a transient mitochondrial Ca^{2+} elevation. The $O_2^{\cdot-}$-induced $[Ca^{2+}]_i$ transient subsequently evoked mitochondrial depolarization independent of mitochondrially derived ROS. In addition to this novel observation, our results suggest that $O_2^{\cdot-}$ selectively evokes Ca^{2+}-dependent $\Delta\Psi_m$ loss independent of other oxidants.

Another important finding is that Tg, but not EGTA, pretreatment eliminated the $O_2^{\cdot-}$-induced increase in $[Ca^{2+}]_i$, indicating release from the ER. We therefore conclude that Ca^{2+} store release in response to $O_2^{\cdot-}$ may be PLC dependent and mediated by $InsP_3R$ on the ER. This conclusion was supported by the observation that DT40 cells lacking all three $InsP_3R$ isoforms failed to show an $[Ca^{2+}]_i$ rise after $O_2^{\cdot-}$ application, unless $InsP_3R$ was reintroduced by transient transfection. Reintroduction of $InsP_3R$ type 1 restored the $[Ca^{2+}]_i$ transient, indicating the existence of the Ca^{2+} signaling machinery in TKO cells. Furthermore, we found that the PLC inhibitor U-73122 blocked the $O_2^{\cdot-}$ response in endothelial cells. PLC normally presents as a key enzyme in cellular metabolism and signaling in response to extracellular agonists by coupling with GTP-binding proteins. DT40 cells express PLC-γ2 and PLC-β isoforms (Rhee, 2001) but lack the GPCRs necessary for PLC-β activation (Venkatachalam et al., 2001; Patterson et al., 2002). Surprisingly, we observed that PLC-γ2 KO cells displayed a rapid $[Ca^{2+}]_i$ store release in response to $O_2^{\cdot-}$, suggesting the activation of PLC-β–mediated Ca^{2+} release by $O_2^{\cdot-}$. PLC inhibition in these PLC-γ2 KO cells by U-73122 indicates activation of PLC and suggests that $O_2^{\cdot-}$-induced $[Ca^{2+}]_i$ rise requires $InsP_3$. Because $InsP_3$ levels were greatly elevated by $O_2^{\cdot-}$ in all three DT40 cell lines, it is apparent that generation of $InsP_3$ by PLC is the essential signal in response to $O_2^{\cdot-}$ for $InsP_3R$ activation. Ca^{2+} release via PLC-β (Liao et al., 1989) was investigated using the G protein–coupled muscarinic M5 receptor agonist carbachol. No detectable Ca^{2+} signals were observed in response to carbachol (500 μM), indicating that DT40 cells lack the GPCR machinery necessary for PLC-β activation (unpublished data). However, we cannot exclude that $O_2^{\cdot-}$ may directly activate signaling upstream of PLC or regulate $InsP_3R$. Earlier, we demonstrated the activation of mitochondrial PLA_2 by $O_2^{\cdot-}$ (Madesh and Balasubramanian, 1997), lending support to our findings on the activation of signaling enzymes by $O_2^{\cdot-}$.

Our findings suggest that $\Delta\Psi_m$ loss in response to $O_2^{\cdot-}$ is dependent on ER stores and not extracellular Ca^{2+}. However, it is unclear whether mitochondrially derived ROS exacerbate Ca^{2+} release from ER stores during oxidative stress. Rotenone and other distal complex I inhibitors generate $O_2^{\cdot-}$ on the matrix side of the inner membrane (Brookes et al., 2004). Our data indicate that cells pretreated with rotenone alone did not trigger either $[Ca^{2+}]_i$ changes or a $\Delta\Psi_m$ change. In contrast, the complex III inhibitor antimycin A caused a sharp decline in the $\Delta\Psi_m$ without concomitant $[Ca^{2+}]_i$ mobilization. This finding suggests that $O_2^{\cdot-}$ generation by complex III directly facilitates $\Delta\Psi_m$ loss independent of $[Ca^{2+}]_i$ levels. Cell death can be initiated by mitochondrial inhibitors through a reduction in ATP levels in a process known as necrosis. Specifically, oligomycin is known to reduce available ATP through inhibition of mitochondrial F_oF_1-ATPase and to elicit cell death through a switch from apoptosis to necrosis. In our system, endothelial cells pretreated with oligomycin did not experience either a rapid $[Ca^{2+}]_i$ change or $\Delta\Psi_m$ decay. However, subsequent delivery of $O_2^{\cdot-}$ perturbed the ER Ca^{2+} level and subsequent $\Delta\Psi_m$ loss. Experiments using the mitochondrial uncoupler FCCP indicate that mitochondrial Ca^{2+} efflux precedes $\Delta\Psi_m$ dissipation. Apparently, mitochondrial depolarization evoked by paracrine $O_2^{\cdot-}$ differs from $\Delta\Psi_m$ alterations induced by mitochondrially derived ROS.

The question arises whether extracellular $O_2^{\cdot-}$ generation evokes selective signaling during endothelial dysfunction. Previously, cells exposed to $O_2^{\cdot-}$ but not H_2O_2 elicited a rapid and large cytochrome *c* release from the mitochondria, followed by $\Delta\Psi_m$ loss (Madesh and Hajnoczky, 2001). Cell death has been associated with elevation of Ca^{2+} through various means. Moreover, elevation of $[Ca^{2+}]_i$ has been implicated in the induction of apoptosis by ROS (Orrenius et al., 2003). It is suggested that H_2O_2 facilitates Ca^{2+} entry from the extracellular milieu or from the intracellular pools (Zhao, 2004), and H_2O_2-induced apoptosis in I/R injury has also been proposed (Inserte et al., 2000). This study suggests that $O_2^{\cdot-}$, but not H_2O_2, evoked an intracellular store Ca^{2+} release that regulates the $\Delta\Psi_m$. Strikingly, pretreatment with the $[Ca^{2+}]_i$ chelator BAPTA-AM prevents $O_2^{\cdot-}$- but not H_2O_2-mediated endothelial $\Delta\Psi_m$ loss. Thus, the $O_2^{\cdot-}$-initiated $\Delta\Psi_m$ loss is dependent on an $[Ca^{2+}]_i$ rise and independent of mitochondrial ROS generation. These findings suggest that extracellularly generated $O_2^{\cdot-}$ rapidly evokes the observed $[Ca^{2+}]_i$ elevation and pathological $\Delta\Psi_m$ loss. Interestingly, we illustrate that externally delivered $O_2^{\cdot-}$, and not other oxidants, triggers a cytosolic signal that initiates the mitochondrial phase of apoptosis.

Mitochondrial membrane permeabilization evoked by apoptotic stimuli facilitate apoptogenic protein release from the intermembrane space and can lead to the downstream activation of both caspase-dependent and -independent apoptotic cascades. Our previous observation proposed that $O_2^{\cdot-}$, but not H_2O_2, elicited cytochrome *c* release via a voltage-dependent anion channel–dependent mitochondrial membrane permeabilization (Madesh and Hajnoczky, 2001). Cytochrome *c* release is regulated by the Bcl-2 family of proteins, and the target of these proteins in the cell is the MPTP (Kroemer and Reed, 2000; Mattson and, Kroemer, 2003). This study shows the activation of initiator and effector caspases by $O_2^{\cdot-}$ specifically, and to some extent, by high doses of H_2O_2. Recent evidence has indicated that a caspase-3–truncated $InsP_3R$ type I may elicit a prolonged $[Ca^{2+}]_i$ elevation during apoptosis (Assefa et al., 2004). Our model indicates that caspase-3 activation is downstream of $[Ca^{2+}]_i$ elevation and $\Delta\Psi_m$ loss. However, we cannot rule out modification of $InsP_3R$ type I in the late stages of $O_2^{\cdot-}$-triggered apoptosis. Collectively, these findings establish that ER Ca^{2+} mobilization is upstream of mitochondrial events evoked by $O_2^{\cdot-}$ in endothelial apoptosis.

In conclusion, activated macrophage-derived $O_2^{\cdot-}$ acts as an important signaling molecule that mediates $InsP_3R$-linked $[Ca^{2+}]_i$ elevation and mitochondrial dysfunction in endothelial cells and provides a novel signaling link between inflammatory and endothelial cells under pathological conditions. We therefore propose that paracrine $O_2^{\cdot-}$ signaling is critical to endothelial cell death.

Materials and methods

Cell culture
Primary rat PMVECs (provided by T. Stevens, University of South Alabama, Mobile, AL) were cultured in DME supplemented with 10% FBS, nonessential amino acids, and antibiotics. Cells of wild-type DT40 chicken B cell line, triple $InsP_3R$ KO cell line (DT40 $InsP_3R$ KO), and PLC-γ2 KO (provided by A. August, Pennsylvania State University, Philadelphia, PA) cell line were cultured in RPMI 1640 supplemented with 10% FCS, 1% chicken serum, 50 μM 2-mercaptoethanol, 4 mM L-glutamine, and antibiotics. J774A.1 monocyte-derived mouse macrophages were cultured in Hank's F12 (supplemented with 10% FBS) and antibiotics. Heptocellular carcinoma cell line (HepG2) was cultured in MEM with 10% FBS, 2 mM L-glutamine, 0.50 mM sodium pyruvate, 0.1 mM nonessential amino acids, and antibiotics. Cells between passages 5 and 10 were used for experiments.

Visualization of ROS generation
J774.1 mouse monocyte-derived macrophages (10^6 cells/ml) were cultured on glass bottom 35-mm dishes (Harvard Apparatus) for 48 h. Cells were challenged with 1 μg/ml LPS for 3 h at 37°C. For DPI treatment, 2.5 h LPS-treated macrophages were incubated with 30 μM DPI for 30 min. The oxidation-sensitive dye H_2DCF-DA (10 μM; Invitrogen) was added separately to dishes 20 min before visualization under confocal microscopy. Macrophage cells treated under similar conditions were used for co-culture model Ca^{2+} mobilization.

$[Ca^{2+}]_i$ measurement
Measurement of $[Ca^{2+}]_i$ changes was performed using the Ca^{2+}-sensitive fluorescent dye Fluo-4/AM (Invitrogen). Cells adherent to 25-mm-diam glass coverslips were incubated at RT in extracellular membrane (ECM) containing 5 μM Fluo-4/AM for 30 min, followed by an additional 10-min incubation in a dye-free medium. Coverslips were affixed to a chamber and mounted in a PDMI-2 open perfusion microincubator (Harvard Apparatus) and maintained at 37°C on an inverted microscope (model TE300; Nikon). Confocal imaging was performed using the Radiance 2000 imaging system (Bio-Rad Laboratories) equipped with a Kr/Ar-ion laser source at 488-nm excitation using a 60× oil objective. Images were collected using LaserSharp software (Bio-Rad Laboratories) every 3 s for $[Ca^{2+}]_i$ changes. Mobilization was induced by the application of 100 μM and 5 mU/ml, respectively, of the xanthine/xanthine oxidase $O_2^{\cdot-}$-generating system. Whole cell masking was used to quantitate individual cell responses (Spectralyzer, custom software; provided by Paul Anderson, Thomas Jefferson University, Philadelphia, PA).

Measurement of inositol phosphates
24 h before experiments, cells (10^6/ml) were transferred to myo-inositol–free DME and incubated in the presence of myo-[2-^{3}H]inositol (2 μCi/ml; 20 Ci/mmol; MP Biomedical, Inc.). After washing with myo-inositol–free DME, cells were incubated for 30 min in myo-inositol–free DME supplemented with 10 mM LiCl and then exposed to either ATP (100 μM) or X+XO (100 μM xanthine and 5 mU/ml XO) for 20 min at 37°C. The medium was subsequently removed and cells were scraped into 1 ml of 10% (wt/vol) TCA for the extraction of soluble inositol phosphates. After centrifugation of the cell lysates, the supernatant was applied to AG 1-X8 (formate form) ion exchange columns (200–400 mesh; Bio-Rad Laboratories). These columns were washed as previously described (Takata et al., 1995). Elution was performed with increasing concentrations of ammonium formate (0.1–0.7 M).

Simultaneous confocal imaging of cytosolic and mitochondrial Ca^{2+} in PMVECs
Endothelial cells were loaded with 2 μM rhod-2/AM in ECM containing 2.0% BSA in the presence of 0.003% pluronic acid at 37°C for 50 min. Cells loaded with rhod-2 dye were washed and then reloaded with Fluo-4/AM for an additional 30 min at RT. Cells were placed on a temperature-controlled stage and images were recorded using the Radiance 2000 imaging system with excitation at 488 and 568 nm for Fluo-4 and rhod-2, respectively.

Kinetics of $[Ca^{2+}]_i$ elevation and mitochondrial membrane depolarization
Cells cultured on 25-mm-diam glass coverslips were loaded for 30 min with 5 μM Fluo-4/AM at RT. The cationic potentiometric fluorescent dye TMRE (100 nM) was added to the loading medium and allowed to equilibrate for at least 15 min. Under these conditions, TMRE fluorescence was largely localized to the mitochondrial matrix space. After dye loading, the cells were washed and resuspended in the experimental imaging solution (ECM containing 0.25% BSA). Intracellular esterase action then resulted in loading of both the cytoplasmic and mitochondrial compartments of the cell. Experiments were performed in ECM containing 0.25% BSA at 37°C. Images were recorded using the Radiance 2000 imaging system with excitation at 488 and 568 nm for Fluo-4 and TMRE, respectively. Fluo-4 and TMRE fluorescent changes were determined by background subtraction followed by masking of total cell area or intracellular regions. During $\Delta\Psi_m$ loss, the exit of TMRE from mitochondria into the cytoplasm leads to quenching of the dye. The rapid redistribution of TMRE into the cytoplasm after depolarization of $\Delta\Psi_m$ can be transiently detected in the nucleus.

Detection of caspase-3, -8, and -9 activity
The assay is based on the ability of the active enzymes to cleave the fluorogenic substrates Ac-DEVD-AFC (caspase-3), Ac-IETD-AFC (caspase-8), or Ac-LEHD-AFC (caspase-9; Calbiochem). Cells treated with various oxidants were harvested via trypsinization and washed with PBS. The cell pellet was gently resuspended in lysis buffer (25 mM Hepes, pH 7.4, 2 mM EDTA, 0.1% CHAPS, 5 mM DTT, 1 mM PMSF, and protease inhibitor cocktail [Roche], lysed, and centrifuged; the supernatant was used as the assay. Caspase substrates were added to a final concentration of 50 μM and the samples were incubated at 37°C for 45 min in caspase assay buffer. Incubated samples were measured at an excitation of 400 nm and an emission of 505 nm in a multiwavelength-excitation dual wavelength-emission fluorimeter (Delta RAM; Photon Technology International).

Confocal imaging analysis of apoptotic markers in PMVECs
To determine cellular outcome in response to oxidative stress, cells were exposed to the $O_2^{\cdot-}$-generating system, H_2O_2, and t-BuOOH for 5 h. To assess the externalization of phosphatidylserine in the plasma membrane, as occurs in the early stage of apoptosis, cells were incubated with the conjugate annexin V Alexa Fluor-488 (Invitrogen) and PI (0.5 μg/ml) for 15 min. After treatment, annexin V– and PI-stained cells were visualized and counted. In normal cells, impermeable PI is internalized as the plasma membrane loses integrity. Thus, positive PI staining indicates either late stage of apoptosis or necrosis.

Data analysis
Tracings are representative of the mean fluorescence value of all cells in one field and are indicative of *n* independent experiments. Data given are representative of duplicate analysis of *n* independent experiments as mean ± SEM.

Online supplemental material
Fig. S1 shows the Ca^{2+} response to the physiological and pathological stimuli ATP and $O_2^{\cdot-}$, respectively, in PMVECs. Fig. S2 details the measurement of $InsP_3$ generation in both DT40 and PMVECs. Fig. S3 shows the analysis of apoptosis in DT40 cells in response to $O_2^{\cdot-}$. Online supplemental material is available at http://www.jcb.org/cgi/content/full/jcb.200505022/DC1.

We thank Drs. Troy Stevens and Avery August for providing endothelial and PLC-γ2 KO cells, respectively. We are grateful to Dr. Kevin Foskett for critical manuscript review. We also thank Drs. Craig Thompson and Sheldon Feinstein for helpful suggestions and Paul Anderson for Spectralyzer image analysis software.

This work was supported by startup funds from the Institute for Environmental Medicine to M. Madesh. A.B. Fisher is funded by National Institutes of Health (NIH) grant HL-60290. S.K. Joseph is supported by NIH grant DK-34804.

Submitted: 4 May 2005
Accepted: 16 August 2005

References

Aon, M.A., S. Cortassa, E. Marban, and B. O'Rourke. 2003. Synchronized whole cell oscillations in mitochondrial metabolism triggered by a local release of reactive oxygen species in cardiac myocytes. *J. Biol. Chem.* 278:44735–44744.

Assefa, Z., G. Bultynck, K. Szlufcik, N. Nadif Kasri, E. Vermassen, J. Goris, L. Missiaen, G. Callewaert, J.B. Parys, and H. De Smedt. 2004. Caspase-3-induced truncation of type 1 inositol trisphosphate receptor accelerates apoptotic cell death and induces inositol trisphosphate-independent calcium release during apoptosis. *J. Biol. Chem.* 279:43227–43236.

Bernardi, P., and V. Petronilli. 1996. The permeability transition pore as a mitochondrial calcium release channel: a critical appraisal. *J. Bioenerg. Biomembr.* 28:131–138.

Berridge, M.J., M.D. Bootman, and P. Lipp. 1998. Calcium—a life and death signal. *Nature.* 395:645–648.

Berridge, M.J., P. Lipp, and M.D. Bootman. 2000. The versatility and universality of calcium signalling. *Nat. Rev. Mol. Cell Biol.* 1:11–21.

Boehning, D., R.L. Patterson, L. Sedaghat, N.O. Glebova, T. Kurosaki, and S.H. Snyder. 2003. Cytochrome c binds to inositol (1,4,5) trisphosphate receptors, amplifying calcium-dependent apoptosis. *Nat. Cell Biol.* 5:1051–1061.

Boitier, E., R. Rea, and M.R. Duchen. 1999. Mitochondria exert a negative feedback on the propagation of intracellular Ca^{2+} waves in rat cortical astrocytes. *J. Cell Biol.* 145:795–808.

Bootman, M.D., T.J. Collins, L. Mackenzie, H.L. Roderick, M.J. Berridge, and C.M. Peppiatt. 2002. 2-aminoethoxydiphenyl borate (2-APB) is a reliable blocker of store-operated Ca^{2+} entry but an inconsistent inhibitor of InsP3-induced Ca^{2+} release. *FASEB J.* 16:1145–1150.

Brookes, P.S., Y. Yoon, J.L. Robotham, M.W. Anders, and S.S. Sheu. 2004. Calcium, ATP, and ROS: a mitochondrial love-hate triangle. *Am. J. Physiol. Cell Physiol.* 287:C817–C833.

Chen, R., I. Valencia, F. Zhong, K.S. McColl, H.L. Roderick, M.D. Bootman, M.J. Berridge, S.J. Conway, A.B. Holmes, G.A. Mignery, et al. 2004. Bcl-2 functionally interacts with inositol 1,4,5-trisphosphate receptors to regulate calcium release from the ER in response to inositol 1,4,5-trisphosphate. *J. Cell Biol.* 166:193–203.

Crompton, M. 1999. The mitochondrial permeability transition pore and its role in cell death. *Biochem. J.* 341:233–249.

Davies, K.J. 1995. Oxidative stress: the paradox of aerobic life. *Biochem. Soc. Symp.* 61:1–31.

Devadas, S., L. Zaritskaya, S.G. Rhee, L. Oberley, and M.S. Williams. 2002. Discrete generation of superoxide and hydrogen peroxide by T cell receptor stimulation: selective regulation of mitogen-activated protein kinase activation and fas ligand expression. *J. Exp. Med.* 195:59–70.

Droge, W. 2002. Free radicals in the physiological control of cell function. *Physiol. Rev.* 82:47–95.

Duchen, M.R. 1992. $Ca^{(2+)}$-dependent changes in the mitochondrial energetics in single dissociated mouse sensory neurons. *Biochem. J.* 283:41–50.

Haimovitz-Friedman, A., C. Cordon-Cardo, S. Bayoumy, M. Garzotto, M. McLoughlin, R. Gallily, C.K. Edwards III, E.H. Schuchman, Z. Fuks, and R. Kolesnick. 1997. Lipopolysaccharide induces disseminated endothelial apoptosis requiring ceramide generation. *J. Exp. Med.* 186:1831–1841.

Hajnoczky, G., E. Davies, and M. Madesh. 2003. Calcium signaling and apoptosis. *Biochem. Biophys. Res. Commun.* 304:445–454.

Hausenloy, D.J., D.M. Yellon, S. Mani-Babu, and M.R. Duchen. 2004. Preconditioning protects by inhibiting the mitochondrial permeability transition. *Am. J. Physiol. Heart Circ. Physiol.* 287:H841–H849.

Houston, M., A. Estevez, P. Chumley, M. Aslan, S. Marklund, D.A. Parks, and B.A. Freeman. 1999. Binding of xanthine oxidase to vascular endothelium. Kinetic characterization and oxidative impairment of nitric oxide-dependent signaling. *J. Biol. Chem.* 274:4985–4994.

Huser, J., C.E. Rechenmacher, and L.A. Blatter. 1998. Imaging the permeability pore transition in single mitochondria. *Biophys. J.* 74:2129–2137.

Inserte, J., G. Taimor, B. Hofstaetter, D. Garcia-Dorado, and H.M. Piper. 2000. Influence of simulated ischemia on apoptosis induction by oxidative stress in adult cardiomyocytes of rats. *Am. J. Physiol. Heart Circ. Physiol.* 278:H94–H99.

Jayaraman, T., and A.R. Marks. 1997. T cells deficient in inositol 1,4,5-trisphosphate receptor are resistant to apoptosis. *Mol. Cell. Biol.* 17:3005–3012.

Johnston, R.B., Jr., C.A. Godzik, and Z.A. Cohn. 1978. Increased superoxide anion production by immunologically activated and chemically elicited macrophages. *J. Exp. Med.* 148:115–127.

Kikuchi, H., M. Hikage, H. Miyashita, and M. Fukumoto. 2000. NADPH oxidase subunit, gp91(phox) homologue, preferentially expressed in human colon epithelial cells. *Gene.* 254:237–243.

Kroemer, G., and J.C. Reed. 2000. Mitochondrial control of cell death. *Nat. Med.* 6:513–519.

Lambeth, J.D. 2004. NOX enzymes and the biology of reactive oxygen. *Nat. Rev. Immunol.* 4:181–189.

Li, C., C.J. Fox, S.R. Master, V.P. Bindokas, L.A. Chodosh, and C.B. Thompson. 2002. Bcl-X(L) affects Ca^{2+} homeostasis by altering expression of inositol 1,4,5-trisphosphate receptors. *Proc. Natl. Acad. Sci. USA.* 99: 9830–9835.

Li, J.M., and A.M. Shah. 2004. Endothelial cell superoxide generation: regulation and relevance for cardiovascular pathophysiology. *Am. J. Physiol. Regul. Integr. Comp. Physiol.* 287:R1014–R1030.

Liao, C.F., A.P. Themmen, R. Joho, C. Barberis, M. Birnbaumer, and L. Birnbaumer. 1989. Molecular cloning and expression of a fifth muscarinic acetylcholine receptor. *J. Biol. Chem.* 264:7328–7337.

Ma, H.T., R.L. Patterson, D.B. van Rossum, L. Birnbaumer, K. Mikoshiba, and D.L. Gill. 2000. Requirement of the inositol trisphosphate receptor for activation of store-operated Ca^{2+} channels. *Science.* 287:1647–1651.

Ma, H.T., K. Venkatachalam, H.S. Li, C. Montell, T. Kurosaki, R.L. Patterson, and D.L. Gill. 2001. Assessment of the role of the inositol 1,4,5-trisphosphate receptor in the activation of transient receptor potential channels and store-operated Ca^{2+} entry channels. *J. Biol. Chem.* 276:18888–18896.

Madesh, M., and K.A. Balasubramanian. 1997. Activation of liver mitochondrial phospholipase A2 by superoxide. *Arch. Biochem. Biophys.* 346:187–192.

Madesh, M., and G. Hajnoczky. 2001. VDAC-dependent permeabilization of the outer mitochondrial membrane by superoxide induces rapid and massive cytochrome *c* release. *J. Cell Biol.* 155:1003–1015.

Malis, C.D., and J.V. Bonventre. 1986. Mechanism of calcium potentiation of oxygen free radical injury to renal mitochondria. A model for post-ischemic and toxic mitochondrial damage. *J. Biol. Chem.* 261:14201–14208.

Mattson, M.P., and G. Kroemer. 2003. Mitochondria in cell death: novel targets for neuroprotection and cardioprotection. *Trends Mol. Med.* 9:196–205.

Orrenius, S., B. Zhivotovsky, and P. Nicotera. 2003. Regulation of cell death: the calcium-apoptosis link. *Nat. Rev. Mol. Cell Biol.* 4:552–565.

Pan, Z., M.B. Bhat, A.L. Nieminen, and J. Ma. 2001. Synergistic movements of Ca^{2+} and Bax in cells undergoing apoptosis. *J. Biol. Chem.* 276:32257–32263.

Parekh, A.B., and R. Penner. 1997. Store depletion and calcium influx. *Physiol. Rev.* 77:901–930.

Patterson, R.L., D.B. van Rossum, D.L. Ford, K.J. Hurt, S.S. Bae, P.G. Suh, T. Kurosaki, S.H. Snyder, and D.L. Gill. 2002. Phospholipase C-gamma is required for agonist-induced Ca^{2+} entry. *Cell.* 111:529–541.

Patterson, R.L., D. Boehning, and S.H. Snyder. 2004. Inositol 1,4,5-trisphosphate receptors as signal integrators. *Annu. Rev. Biochem.* 73:437–465.

Pinton, P., D. Ferrari, P. Magalhaes, K. Schulze-Osthoff, F. Di Virgilio, T. Pozzan, and R. Rizzuto. 2000. Reduced loading of intracellular Ca^{2+} stores and downregulation of capacitative Ca^{2+} influx in Bcl-2–overexpressing cells. *J. Cell Biol.* 148:857–862.

Putney, J.W., Jr., and G.S. Bird. 1993. The signal for capacitative calcium entry. *Cell.* 75:199–201.

Ran, Q., H. Liang, M. Gu, W. Qi, C.A. Walter, L.J. Roberts II, B. Herman, A. Richardson, and H. Van Remmen. 2004. Transgenic mice overexpressing glutathione peroxidase 4 are protected against oxidative stress-induced apoptosis. *J. Biol. Chem.* 279:55137–55146.

Rhee, S.G. 2001. Regulation of phosphoinositide-specific phospholipase C. *Annu. Rev. Biochem.* 70:281–312.

Rizzuto, R., P. Pinton, W. Carrington, F.S. Fay, K.E. Fogarty, L.M. Lifshitz, R.A. Tuft, and T. Pozzan. 1998. Close contacts with the endoplasmic reticulum as determinants of mitochondrial Ca^{2+} responses. *Science.* 280:1763–1766.

Sugawara, H., M. Kurosaki, M. Takata, and T. Kurosaki. 1997. Genetic evidence for involvement of type 1, type 2 and type 3 inositol 1,4,5-trisphosphate receptors in signal transduction through the B-cell antigen receptor. *EMBO J.* 16:3078–3088.

Takata, M., Y. Homma, and T. Kurosaki. 1995. Requirement of phospholipase C-γ2 activation in surface immunoglobulin M–induced B cell apoptosis. *J. Exp. Med.* 182:907–914.

Turrens, J.F., A. Alexandre, and A.L. Lehninger. 1985. Ubisemiquinone is the electron donor for superoxide formation by complex III of heart mitochondria. *Arch. Biochem. Biophys.* 237:408–414.

Venkatachalam, K., H.T. Ma, D.L. Ford, and D.L. Gill. 2001. Expression of functional receptor-coupled TRPC3 channels in DT40 triple receptor InsP3 knockout cells. *J. Biol. Chem.* 276:33980–33985.

Warren, M.C., E.A. Bump, D. Medeiros, and S.J. Braunhut. 2000. Oxidative stress-induced apoptosis of endothelial cells. *Free Radic. Biol. Med.* 29:537–547.

Wei, M.C., W.X. Zong, E.H. Cheng, T. Lindsten, V. Panoutsakopoulou, A.J.

Ross, K.A. Roth, G.R. MacGregor, C.B. Thompson, and S.J. Korsmeyer. 2001. Proapoptotic BAX and BAK: a requisite gateway to mitochondrial dysfunction and death. *Science.* 292:727–730.

Wei, Z., K. Costa, A.B. Al-Mehdi, C. Dodia, V. Muzykantov, and A.B. Fisher. 1999. Simulated ischemia in flow-adapted endothelial cells leads to generation of reactive oxygen species and cell signaling. *Circ. Res.* 85:682–689.

White, C., C. Li, J. Yang, N.B. Petrenko, M. Madesh, C.B. Thompson, and J. Kevin Foskett. 2005. The endoplasmic reticulum gateway to apoptosis: Bcl-XL modulation of the $InsP_3$ receptor. *Nat. Cell Biol.* In press.

Zeng, W., D.O. Mak, Q. Li, D.M. Shin, J.K. Foskett, and S. Muallem. 2003. A new mode of Ca^{2+} signaling by G protein-coupled receptors: gating of IP3 receptor Ca^{2+} release channels by Gbetagamma. *Curr. Biol.* 13: 872–876.

Zhao, Z.Q. 2004. Oxidative stress-elicited myocardial apoptosis during reperfusion. *Curr. Opin. Pharmacol.* 4:159–165.

Zong, W.X., C. Li, G. Hatzivassiliou, T. Lindsten, Q.C. Yu, J. Yuan, and C.B. Thompson. 2003. Bax and Bak can localize to the endoplasmic reticulum to initiate apoptosis. *J. Cell Biol.* 162:59–69.

Zorov, D.B., C.R. Filburn, L.O. Klotz, J.L. Zweier, and S.J. Sollott. 2000. Reactive oxygen species (ROS)-induced ROS release: a new phenomenon accompanying induction of the mitochondrial permeability transition in cardiac myocytes. *J. Exp. Med.* 192:1001–1014.